

Constraints on the threshold K^- nuclear potential from FINUDA ${}^A Z(K^-_{\text{stop}}, \pi^-) {}^A Z$ spectra

A. Cieplý^a, E. Friedman^b, A. Gal^{b,*}, V. Krejčíř^{a,c}

^a*Nuclear Physics Institute, 25068 Řež, Czech Republic*

^b*Racah Institute of Physics, The Hebrew University, 91904 Jerusalem, Israel*

^c*Department of Physics, University of Maryland, College Park, MD 20742-4111, USA*

Abstract

$1s_\Lambda$ hypernuclear formation rates in stopped K^- reactions on several p -shell targets are derived from hypernuclear formation spectra measured recently by the FINUDA Collaboration and are compared with calculated $1s_\Lambda$ formation rates. It is shown that the A dependence of these derived rates constrains the depth of the threshold K^- nuclear potential, favoring a shallow potential of depth about 50 MeV.

Keywords: hypernuclei, kaon-induced reactions, mesonic atoms

PACS: 21.80.+a, 25.80.Nv, 36.10.Gv

1. Introduction

How strong is the K^- nuclear interaction? Various scenarios proposed for kaon condensation in dense neutron-star matter [1], and more recently for quasibound K^- nuclear clusters [2] and for self-bound strange hadronic matter [3] depend on the answer to this question which has not been resolved todate. A modern theoretical framework for the underlying low-energy $\bar{K}N$ interaction is provided by the leading-order Tomozawa-Weinberg (TW) vector term of the chiral effective Lagrangian which, in Born approximation, yields a sizable attraction for the \bar{K} -nuclear potential $V_{\bar{K}}$:

$$V_{\bar{K}} = -\frac{3}{8f_\pi^2} \rho \sim -55 \frac{\rho}{\rho_0} \text{ MeV} \quad (1)$$

*Corresponding author: Avraham Gal, avragal@vms.huji.ac.il

for $\rho_0 = 0.16 \text{ fm}^{-3}$, where $f_\pi \sim 93 \text{ MeV}$ is the pseudoscalar meson decay constant. This attraction is doubled, roughly, within a unitarized coupled-channel $\bar{K}N - \pi\Sigma - \pi\Lambda$ calculation which provides also for a strong absorptivity [4]. Shallower potentials, with $\text{Re}V_{\bar{K}}(\rho_0) \sim -(40 - 60) \text{ MeV}$, are obtained by imposing a Watson-like self-consistency requirement on the nuclear-medium $\bar{K}N$ $t(\rho)$ matrix that enters the optical potential $V_{\bar{K}} = t(\rho)\rho$ [5, 6]. In contrast, comprehensive global fits to K^- -atom strong-interaction shifts and widths yield extremely deep density dependent optical potentials at threshold, in the range $\text{Re}V_{\bar{K}}(\rho_0) \sim -(150 - 200) \text{ MeV}$ [7]. It is our purpose in this Letter to discuss recent FINUDA measurements that bear on this issue and to demonstrate their relevance for constraining the strength of the threshold K^- nuclear attraction.

In the preceding Letter [8], the FINUDA Collaboration at DAΦNE, Frascati, reported on Λ -hypernuclear spectra taken in the $K_{\text{stop}}^- + {}^A\text{Z} \rightarrow \pi^- + {}^A_\Lambda\text{Z}$ reaction on several p -shell nuclear targets. Formation rates were given per stopped K^- , mostly in the bound state region. These rates agree, for ${}^{16}_\Lambda\text{O}$, with a previous KEK measurement [9], but are higher than those provided by past DWIA calculations [10, 11, 12]. The calculated rates for a given target exhibit sensitivity to the outgoing pion absorption which is particularly strong for Λ hypernuclear formation occurring kinematically below but sufficiently close to the (3,3) resonance. However, the A dependence of the formation rates is expected to display lesser sensitivity to the pion optical potential used in the DWIA calculation. The recent FINUDA data allow for the first time to consider the A dependence of the formation rates in detail within the nuclear p shell where nuclear structure effects may be reliably separated out. It is our purpose in this companion Letter to apply one's knowledge of the nuclear structure aspect of the problem in order to extract the dynamical contents of the measured formation rates, particularly that part which concerns the K^- nuclear dynamics at threshold. In doing so we transform the partial formation rates reported [8] for well defined and spectroscopically reliable final Λ hypernuclear states into $1s_\Lambda$ hypernuclear formation rates that allow direct comparison with recent DWIA calculations [12]. A typical DWIA amplitude is given by

$$T_{fi}^{\text{DWIA}}(\mathbf{q}_f) = \int d^3r \chi_{\mathbf{q}_f}^{(-)*}(\mathbf{r}) \rho_{fi}(\mathbf{r}) \Psi_{nLM}(\mathbf{r}), \quad (2)$$

where ρ_{fi} stands for the nuclear to hypernuclear transition form factor, $\chi_{\mathbf{q}_f}^{(-)}$ is an outgoing pion distorted wave generated by a pion optical potential fitted to

scattering data, and Ψ_{nLM} is a K^- -atomic wavefunction obtained by solving the Klein-Gordon equation with a K^- -nuclear strong interaction potential $V_{\bar{K}}$ added to the appropriate Coulomb potential. The integration on the r.h.s. of Eq. (2) is confined by the bound-state form factor ρ_{fi} to within the nucleus, where Ψ_{nLM} is primarily determined by the strong-interaction $V_{\bar{K}}$, in spite of Ψ_{nLM} being an atomic wavefunction that peaks far outside the nucleus. Assuming that ρ_{fi} and $\chi_{\mathbf{q}_f}^{(-)}$ are under fair phenomenological control, it is the initial-state dynamical contents due to Ψ_{nLM} that is revealed by studying the A dependence of the $1s_\Lambda$ formation rates in K^- capture at rest. It is shown in the present work that the A dependence of the $1s_\Lambda$ formation rates in K^- capture at rest is a sensitive measure of the depth of the threshold K^- nuclear potential and that the A dependence of the $1s_\Lambda$ rates derived from the FINUDA data favors a shallow potential over a very deep one.

2. Derivation of $1s_\Lambda$ capture rates from FINUDA data

The FINUDA spectra show distinct peaks for several $1s_\Lambda$ and $1p_\Lambda$ states in the nuclear p shell. In general, the derivation of the $1p_\Lambda$ formation rate is ambiguous given that the $1p_\Lambda$ formation strength is often obscured by a rising Λ continuum. In ${}^9_\Lambda\text{Be}$ and in ${}^{13}_\Lambda\text{C}$ it is also mixed with a substantial part of the $1s_\Lambda$ formation strength owing particularly to high lying $T = 1$ parents in the corresponding core nuclei. For this reason, we here deal only with the $1s_\Lambda$ formation strength, attempting to derive it from an unambiguous identification of *low lying* $1s_\Lambda$ hypernuclear states. For such states we use the theoretical framework of Ref. [13] in which hypernuclear formation rates are expressed in terms of a $1s_\Lambda$ formation rate, which is independent of the particular hypernuclear state, times a structure fraction which is derived from neutron pick-up spectroscopic factors in the target nucleus. This theoretical framework is also applicable to forward cross sections of in-flight reactions such as (π^+, K^+) and $(e, e'K^+)$. In Table 1 we present $1s_\Lambda$ formation rates derived from the FINUDA K^- capture at rest hypernuclear spectra [8, 14] for a procedure denoted (a). In each spectrum we focus on the strongest low-lying particle-stable hypernuclear excitation which is also well described in terms of a Λ hyperon weakly coupled to a nuclear core parent state. These core parent states are specified in the table. The measured formation rates are then divided by the corresponding structure fractions to obtain $1s_\Lambda$ formation rates. For comparison, we display in the last column the $1s_\Lambda$ component of forward-angle integrated (π^+, K^+) cross sections (KEK-E336 [16]) derived

using the peaks listed in the second and third columns. These (π^+, K^+) strengths show little A dependence, in contrast to the K^- capture at rest $1s_\Lambda$ formation rates that decrease by a factor 3.5 in going from ${}^7\text{Li}$ to ${}^{16}\text{O}$.

Table 1: $1s_\Lambda$ formation rates in K^- capture at rest on p shell nuclei derived from the strongest hypernuclear bound state peak in each of the listed targets [procedure (a)]. Data are taken from the preceding Letter [8], except for ${}^{12}_\Lambda\text{C}$ [14]. The $1s_\Lambda$ structure fractions are from [15] and, if unlisted there, from [13]. Listed in the last column, for comparison, are $1s_\Lambda$ forward-angle integrated (π^+, K^+) cross sections, derived also by using procedure (a) from KEK-E336 measurements [16].

target AZ	peak J_{core}^π	E_{core}^* (MeV)	$1s_\Lambda$ frac.	$R(1s_\Lambda) \times 10^3$ per stopped K^-	$\sigma_{1s_\Lambda}(\mu b)$ (π^+, K^+)
${}^7\text{Li}$	3^+	2.19	0.311	$1.48 \pm 0.16 \pm 0.19$	1.56 ± 0.10
${}^9\text{Be}$	2^+	2.94	0.242	$0.87 \pm 0.08 \pm 0.12$	1.40 ± 0.05
${}^{12}\text{C}$	$(3/2)^-$	g.s.	0.810	$1.25 \pm 0.14 \pm 0.12$	1.78 ± 0.04
${}^{13}\text{C}$	2^+	4.44	0.224	$0.85 \pm 0.09 \pm 0.13$	1.87 ± 0.09
${}^{16}\text{O}$	$(3/2)^-$	6.18	0.618	$0.42 \pm 0.06 \pm 0.06$	1.47 ± 0.05

In the second procedure, denoted (b) and presented in Table 2, we consider all the particle-stable $1s_\Lambda$ states corresponding to observed peaks for which the shell model offers reliable identification. For three of the five targets listed, this procedure saturates or is close to saturating the $1s_\Lambda$ formation strength. However, in both ${}^9_\Lambda\text{Be}$ and ${}^{13}_\Lambda\text{C}$ the $1s_\Lambda$ particle stable hypernuclear states represent less than half of the full $1s_\Lambda$ strength. In passing we remark that in ${}^{13}_\Lambda\text{C}$ we have ignored the third peak at 7.6 MeV excitation, apparently based on the 0^+ ‘Hoyle state’ in ${}^{12}\text{C}$, because the shell model fails to explain it in natural terms. Similarly to Table 1, in the last column of Table 2 we assembled $1s_\Lambda$ forward-angle integrated (π^+, K^+) cross sections, derived from KEK-E336 measurements [16] by applying here procedure (b). The very weak A dependence of these $1s_\Lambda$ (π^+, K^+) cross sections, again, is in stark contrast to the fast decrease of the $1s_\Lambda$ formation rates by a factor 3.5, going from ${}^7\text{Li}$ to ${}^{16}\text{O}$, in K^- capture at rest.

Comparing the two procedures (a) and (b) in Tables 1 and 2, it is encouraging to see that both of these procedures yield very similar values for the $1s_\Lambda$ formation strength in each one of the nuclear targets studied. If only statistical uncertainties are considered (the first listed), then this statement holds for the four spectra of the recent run [8], but not for ${}^{12}_\Lambda\text{C}$ from the older

Table 2: $1s_\Lambda$ formation rates in K^- capture at rest on p shell nuclei derived from several reliable $1s_\Lambda$ bound states [procedure (b)]. Data are taken from the preceding Letter [8], except for $^{12}_\Lambda\text{C}$ [14]. The $1s_\Lambda$ structure fractions are from [15] and, if unlisted there, from [13]. Listed in the last column, for comparison, are $1s_\Lambda$ forward-angle integrated (π^+ , K^+) cross sections, derived also by using procedure (b) from KEK-E336 measurements [16].

target AZ	peaks	$1s_\Lambda$ frac.	$R(1s_\Lambda) \times 10^3$ per stopped K^-	$\sigma_{1s_\Lambda}(\mu b)$ (π^+ , K^+)
^7Li	1,2,3	0.833	$1.25 \pm 0.14 \pm 0.17$	1.29 ± 0.12
^9Be	1,2	0.435	$0.85 \pm 0.09 \pm 0.11$	1.20 ± 0.05
^{12}C	1,2,3	0.995	$1.67 \pm 0.23 \pm 0.23$	1.92 ± 0.07
^{13}C	1,2	0.347	$0.84 \pm 0.12 \pm 0.12$	1.93 ± 0.12
^{16}O	1,2	1.000	$0.36 \pm 0.06 \pm 0.05$	1.32 ± 0.05

run [14]. For subsequent use, we focus on the $1s_\Lambda$ formation rates extracted under procedure (a).

3. Confronting data with DWIA calculations

The $1s_\Lambda$ formation rates derived from the FINUDA K^- capture at rest spectra [8, 14] by applying procedure (a), and listed in Table 1, are plotted in Fig. 1 together with $1s_\Lambda$ rates calculated for a shallow K^- nuclear potential K_χ of depth $-\text{Re } K_\chi(\rho = \rho_0) \approx 50$ MeV and for a deep potential K_{DD} of depth $-\text{Re } K_{\text{DD}}(\rho = \rho_0) \approx 190$ MeV, using a pion optical potential denoted π_b .¹ Other pion optical potentials tested by us lead to lower calculated formation rates, thus worsening the disagreement between calculation and experiment. The figure confirms past experience that the calculated rates [10, 11, 12, 6] are generally lower than those derived from measurements [9, 14, 17], and that the deeper the K^- potential, the worse is the disagreement [6].

We focus now on the A dependence of the $1s_\Lambda$ formation rates, scaling up the calculated rates by a fixed normalization for given K^- and π^- potentials, in order to achieve agreement for ^7Li with the $1s_\Lambda$ rate derived from the data under procedure (a) in Table 1. This is shown in Fig. 2 where the uncertainties of the experimentally derived $1s_\Lambda$ rates consist only of statistical errors

¹The rates given in Ref. [12] have been recalculated with refined K^- and π^- wave functions, and are updated here.

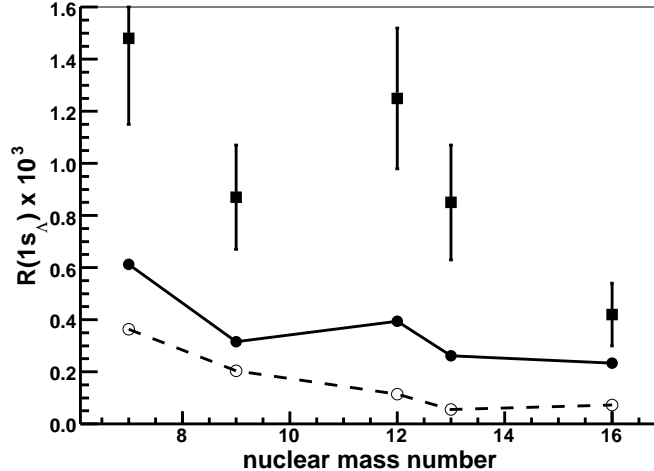


Figure 1: $1s_\Lambda$ formation rates in K^- capture at rest on p shell nuclei, derived from recent FINUDA data [8] and for ^{12}C from older FINUDA data [14] using procedure (a) as listed in Table 1, and as calculated for a shallow K^- nuclear potential K_χ (solid line) and for a deep potential K_{DD} (dashed line) using the pion optical potential π_b [12]. The error bars correspond to the summed statistical and systematic uncertainties of the reported rates. The lines connecting calculated rates are drawn to guide the eye.

that vary from one target to another. The systematic errors, on the other hand, are the same for all targets and drop out when considering A dependence within the present set of FINUDA data. The normalized calculated $1s_\Lambda$ rates shown in the figure are for pion optical potentials π_b and π_e , and for the K^- nuclear potentials K_χ and K_{DD} (for which the absolute rates using π_b are displayed in Fig. 1). We note that the decrease of the experimentally derived $1s_\Lambda$ rates from ^7Li to ^9Be is well reproduced by all of the four calculations shown in Fig. 2 but only the shallow K_χ calculated rates, irrespective of the pion optical potential used, follow reasonably well the A dependence of the experimentally derived rates from ^9Be on. In contrast, the K_{DD} calculated rates drop off too fast as a function of A and are unable to reproduce the nonmonotonic behavior of the experimentally derived rates around ^{12}C . It is evident from the figure that the dependence of the normalized calculated rates on the type of K^- nuclear potential, shallow or deep, is stronger than the dependence on the pion optical potential for a fixed K^- potential. We remark that of the two pion optical potentials used here, π_e provides by far

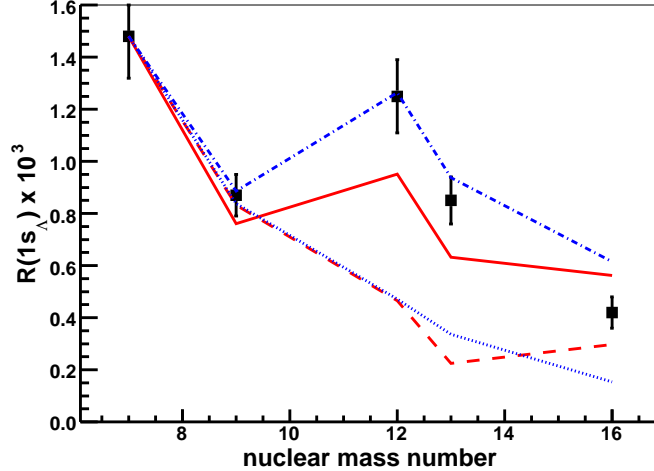


Figure 2: Comparison between $1s_\Lambda$ formation rates derived from the FINUDA K^- capture at rest data [8, 14] and DWIA calculations normalized to the $1s_\Lambda$ formation rate of ${}^7_\Lambda\text{Li}$ listed in Table 1. The Calculated $1s_\Lambda$ formation rates use two pion optical potentials, π_b [12] (in red; solid and dashed lines) and π_e [6] (in blue; dash-dotted and dotted lines), and two K^- nuclear potentials, a shallow K_χ (solid and dash-dotted upper group of lines) and a deep K_{DD} (dashed and dotted lower group of lines). The error bars consist of statistical uncertainties alone.

a better fit to measured $\pi^- - {}^{12}\text{C}$ angular distributions at 162 MeV [6].

In Table 3 we show the ratio of calculated $1s_\Lambda$ formation rates in ${}^7\text{Li}$ to ${}^{16}\text{O}$, for each one of the K^- nuclear potentials K_χ and K_{DD} and for the three pion optical potentials π_b , π_c [12] and π_e [6], comparing this ratio with that for the experimentally derived $1s_\Lambda$ formation rates. In ${}^7\text{Li}$ the stopped K^- meson is absorbed dominantly from $L = 1$ atomic states here represented by a $2p$ atomic wavefunction, whereas in ${}^{16}\text{O}$ it is absorbed dominantly from $L = 2$ atomic states represented by a $3d$ atomic wavefunction. This shift from $2p$ absorption to $3d$ absorption offers maximal sensitivity to the type of the K^- nuclear potential which generates these atomic wavefunctions. It is clear from the table that the sensitivity of the ratio $R(1s_\Lambda)[{}^7\text{Li}]/R(1s_\Lambda)[{}^{16}\text{O}]$ to the pion optical potential used is remarkably weak for the K_χ potential. This observation is correlated with the nodeless structure of the $2p$ and $3d$ atomic K^- wavefunctions for ${}^7\text{Li}$ and ${}^{16}\text{O}$, respectively. The K_χ calculated values for $R(1s_\Lambda)[{}^7\text{Li}]/R(1s_\Lambda)[{}^{16}\text{O}]$ are lower by one standard deviation than

Table 3: Ratio of $R(1s_\Lambda)[{}^7\text{Li}]$ to $R(1s_\Lambda)[{}^{16}\text{O}]$, derived from FINUDA data [8] under procedure (a) in Table 1, and as calculated using pion optical potentials π_b , π_c [12] and π_e [6] for both shallow K_χ and deep K_{DD} K^- nuclear potentials. Listed in the last column, for comparison, is the ${}^7\text{Li}$ to ${}^{16}\text{O}$ ratio of $1s_\Lambda$ forward-angle integrated (π^+, K^+) cross sections, derived also by using procedure (a) from KEK-E336 measurements [16].

V_{K^-}	$R(1s_\Lambda)[{}^7\text{Li}]/R(1s_\Lambda)[{}^{16}\text{O}]$				$\sigma_{1s_\Lambda}[{}^7\text{Li}]/\sigma_{1s_\Lambda}[{}^{16}\text{O}]$ (π^+, K^+)
	π_b	π_c	π_e	exp.	
K_χ	2.63	2.81	2.41	3.52 ± 0.88	1.06 ± 0.10
K_{DD}	4.97	8.00	9.68	3.52 ± 0.88	1.06 ± 0.10

the ratio derived from the FINUDA data. It is also clear from the table that for the K_{DD} potential the sensitivity of the ratio $R(1s_\Lambda)[{}^7\text{Li}]/R(1s_\Lambda)[{}^{16}\text{O}]$ to the pion optical potential used is considerably stronger, and this observation too may be correlated with the node structure of the atomic K^- wavefunctions that enhances the sensitivity to the oscillating pion distorted waves in the $(K_{\text{stop}}^-, \pi^-)$ DWIA amplitude Eq. (2). The K_{DD} calculated values for $R(1s_\Lambda)[{}^7\text{Li}]/R(1s_\Lambda)[{}^{16}\text{O}]$ are all substantially higher than the ratio derived from the FINUDA data.

4. Conclusion

In conclusion, we have derived $1s_\Lambda$ hypernuclear formation rates from peak formation rates associated with the ${}^A\text{Z}(K_{\text{stop}}^-, \pi^-)_{\Lambda}^A\text{Z}$ spectra presented recently by the FINUDA Collaboration on several nuclear targets in the p shell [8, 14]. We then compared the A dependence of these derived rates with that provided by calculations for the two extreme $V_{\bar{K}}$ scenarios discussed at present, a chiral shallow potential and a density dependent deep potential. The calculations demonstrate a strong sensitivity to the K^- nuclear potential at threshold through the atomic wavefunctions it generates and which enter into the DWIA calculation of the formation rates in stopped K^- reactions. The sensitivity to the pion distortion through the pion optical potential used is secondary when studying the A dependence of the calculated $1s_\Lambda$ hypernuclear formation rates. The comparison between the calculated A dependence and that derived from the FINUDA data favors a shallow K^- nuclear potential over a very deep one. In future work, it would be interesting to extend the range of nuclear targets used in stopped K^- reactions to medium and

heavy weight nuclei in order to confirm the present conclusion and to look for more subtle effects of density dependence.

Acknowledgements

We are grateful to Tullio Bressani and Germano Bonomi for useful discussions of the FINUDA measurements. This work was supported by the GAUK Grant No. 91509 and the GACR Grant No. 202/09/1441, as well as by the EU initiative FP7, HadronPhysics2, under Project No. 227431.

References

- [1] B.D. Kaplan, A.E. Nelson, Phys. Lett. B **175** (1986) 57; Phys. Lett. B **179** (1986) 409.
- [2] Y. Akaishi, T. Yamazaki, Phys. Rev. C **65** (2002) 044005.
- [3] D. Gazda, E. Friedman, A. Gal, J. Mareš, Phys. Rev. C **76** (2007) 055204, **77** (2008) 045206, **80** (2009) 035205.
- [4] W. Weise, R. Härtle, Nucl. Phys. A **804** (2008) 173 and references therein.
- [5] A. Ramos, E. Oset, Nucl. Phys. A **671** (2000) 481.
- [6] A. Cieplý, E. Friedman, A. Gal, J. Mareš, Nucl. Phys. A **696** (2001) 173.
- [7] E. Friedman, A. Gal, Phys. Rep. **452** (2007) 89, and references therein.
- [8] M. Agnello, et al. [FINUDA Collaboration], submitted to Phys. Lett. B [arXiv:1011.2695 (nucl-ex)].
- [9] H. Tamura, R.S. Hayano, H. Outa, T. Yamazaki, Prog. Theor. Phys. Suppl. **117** (1994) 1.
- [10] A. Gal, L. Klieb, Phys. Rev. C **34** (1986) 956.
- [11] A. Matsuyama, K. Yazaki, Nucl. Phys. A **477** (1988) 673.
- [12] V. Krejčířík, A. Cieplý, A. Gal, Phys. Rev. C **82** (2010) 024609.

- [13] R.H. Dalitz, A. Gal, Ann. Phys. **116** (1978) 167.
- [14] M. Agnello, et al. [FINUDA Collaboration], Phys. Lett. B **622** (2005) 35.
- [15] D.J. Millener, A. Gal, C.B. Dover, R.H. Dalitz, Phys. Rev. C **31** (1985) 499.
- [16] O. Hashimoto, H. Tamura, Prog. Part. Nucl. Phys. **57** (2006) 564.
- [17] A.W. Ahmed, et al., Phys. Rev. C **68** (2003) 064004.